# The Empirical Angular Function Approach: Testing Sea Surface Temperature Satellite Retrievals

ALEKSANDR M. IGNATOV AND G. GARIK GUTMAN

*NOAA/NESDIS, Satellite Research Laboratory, Camp Springs, Maryland*

1 June 1994 and 30 January 1995

ABSTRACT

Recently, a statistical procedure was proposed to analyze the angular effect in the NOAA Advanced Very High Resolution Radiometer (AVHRR) brightness temperatures. The estimated empirical angular functions (EAF) over the oceans allow one to check the algorithms for the sea surface temperature (SST) and the column water vapor content when the observation geometry is variable, as well as to test angular methods of SST retrieval. The EAF approach has been previously applied to the analysis of the AVHRR brightness temperatures in channels 3 and 4 and dual-window SST over the tropical Atlantic in June 1987 and December 1988 from *NOAA-10* and *NOAA-11*, respectively. Here, it is extended to estimate the accuracy of the split-window sea surface temperature and atmospheric water vapor retrievals from *NOAA-9* over the tropical and North Atlantic in July 1986. The authors confirm the previously drawn conclusion that in a general case no angle-independent coefficients in a linear SST retrieval algorithm can provide angle-invariant retrievals. More recent operational NOAA angle-dependent algorithms have been shown to improve retrievals in the Tropics. In high latitudes, they seem to slightly overcorrect the angular effect. Using satellite data of higher spatial resolution with better radiometric accuracy is expected to improve the accuracy of the EAFs and the reliability of the conclusions.

## 1. Introduction

The Advanced Very High Resolution Radiometer (AVHRR) on board National Oceanic and Atmospheric Administration (NOAA) satellites observes the underlying surface at different viewing angles within $\Theta \approx \pm 68°$ around nadir ($\Theta$ is defined as zenith angle of the satellite as viewed from the surface). The algorithms for retrieval of the sea surface temperature (SST), $t_s$, and atmospheric integral water vapor content $W$ from the angle-dependent brightness temperatures (BT) $t_i(\Theta)$ ($i = 4$ and 5 for AVHRR channels 4 and 5 with central wavelengths $\lambda = 10.8$ and 12 $\mu$m, respectively) should account for $\Theta$ to provide a result invariant of the variable observation geometry. Recently, Ignatov and Dergileva (1994) (hereafter ID94) proposed a statistical method to assess the magnitude of the angular effect in both the original AVHRR BTs and the retrieved SST. It was applied to evaluate the dual-window SST over the tropical Atlantic from *NOAA-10* (June 1987) and *NOAA-11* (December 1988). In the present paper, we use that approach to estimate the angular effect in the split-window BTs, SST, and $W$ from *NOAA-9* (July 1986) over the same target in the tropical Atlantic, and an additional target in the North Atlantic. Also, we test the angular method of the SST retrieval proposed by Saunders (1967), Gorodetsky (1981), and Chedin et al. (1982).

## 2. Concept of the empirical angular function

Brightness temperature in the $i$th channel $t_i(\mathbf{s}; \Theta)$ under cloud-free conditions depends upon the state of the ocean–atmosphere system (vector $\mathbf{s}$) and the observation geometry (angle $\Theta$). If the ocean and atmosphere were constant ($\mathbf{s} = \text{const}$), then BT would depend only on geometrical factor; that is, $t_i(\mathbf{s}; \Theta) \equiv t_i(\Theta)$. We define that dependence as an angular function. Modeling the angular function is rather straightforward, once a radiative transfer model and surface and atmospheric parameters are chosen. The derivation of the empirical angular function EAF at the top of the atmosphere, however, is a challenge since it requires observations of a target with a constant SST through a constant atmosphere at many viewing angles $\Theta_k$, $k = 1, \cdots, K$.

Antoine et al. (1992) proposed to look at the same point on the ocean surface from two consecutive NOAA orbits. That is possible only outside the tropical regions, where the NOAA orbits overlap. Testing of the atmospheric correction algorithms, however, is preferable in the Tropics because atmospheric effects are strongest there. Even in high latitudes, the method of Antoine et al. (1992) can attain BTs only at a few viewing angles, and those few only determined by the satellite orbital geometry. Additionally, errors of dif-

*Corresponding author address:* Dr. Aleksandr M. Ignatov, NOAA/NESDIS-E/RA11, NSC Rm. 711, 5200 Auth Rd., Camp Springs, MD 20746.

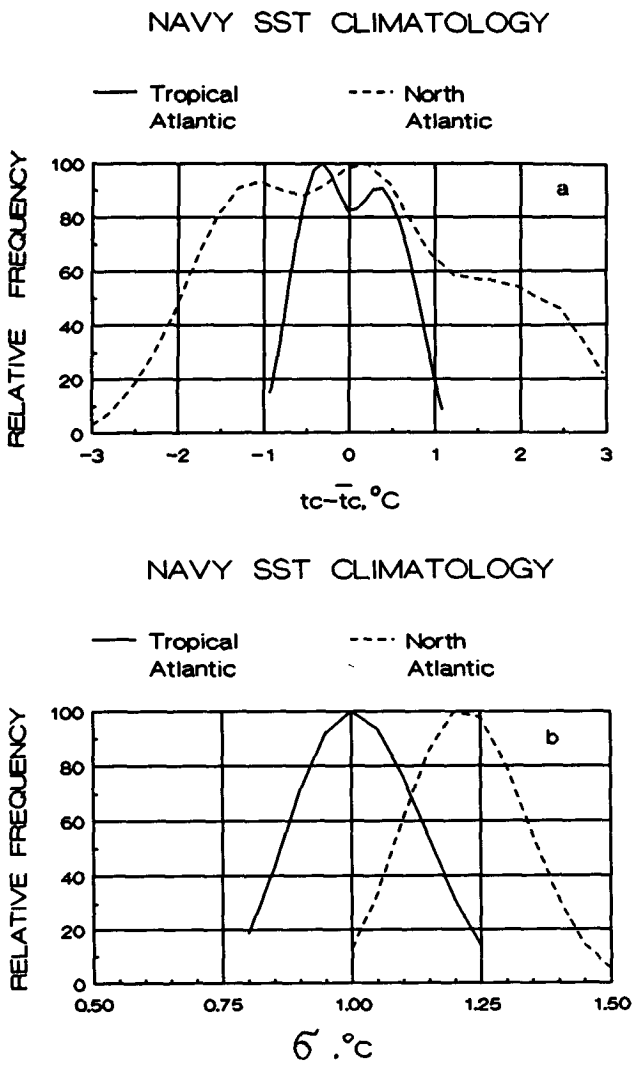


FIG. 1. Histograms of the climatic $(1°)^2$ SST over the two regions centered about the respective (a) means and (b) standard deviations (U.S. Navy 1992).

ferent nature such as partial cloudiness, variability of the ocean, and atmosphere between the two consecutive satellite overpasses, noise in satellite BTs, and navigation errors might have a crucial impact on the results. The approach of Antoine et al. (1992) is somewhat similar to that of Chedin et al. (1982) and Holyer (1984), who observed the same target from two different satellites—NOAA and Meteosat (GOES), except the latter method has an additional source of error resulting from intercalibration of different satellite sensors. The Along Track Scanning Radiometer (ATSR) on board the European research satellite *ERS-1* allows viewing any target on the earth's surface at two angles $\Theta_1 \approx 0°$ and $\Theta_2 \approx 55°$, from two consecutive points of the orbit. It alleviates partially, but not completely, the problems inherent to the above two approaches.

The statistical procedure proposed in ID94 allows one to estimate the EAFs in the full range of the AVHRR viewing angles and does not pose any geographical restrictions. It is based on a histogram analysis of satellite data collected over a large quasi-uniform ocean region $S \sim (10°)^2$, which is stable enough during the time $\tau \sim 1$ month to allow multiple observations of $S$ at different viewing angles. The histograms of BTs are constructed using all satellite measurements over the $(S, \tau)$ but separately for different angle bins $\Delta_k \equiv (\Theta_k, \Theta_k + \Delta\Theta_k)$. The warm quasi-Gaussian peak is associated with clear-sky views (Smith et al. 1970; Crosby and Glasser 1978), and its mode $\bar{t}(\Theta_k)$—the mathematical expectation of the BT over the $(S, \tau, \Delta_k)$ domain—corresponds to the mean ocean–atmospheric condition $\bar{s}$. Estimation of the modes of his-

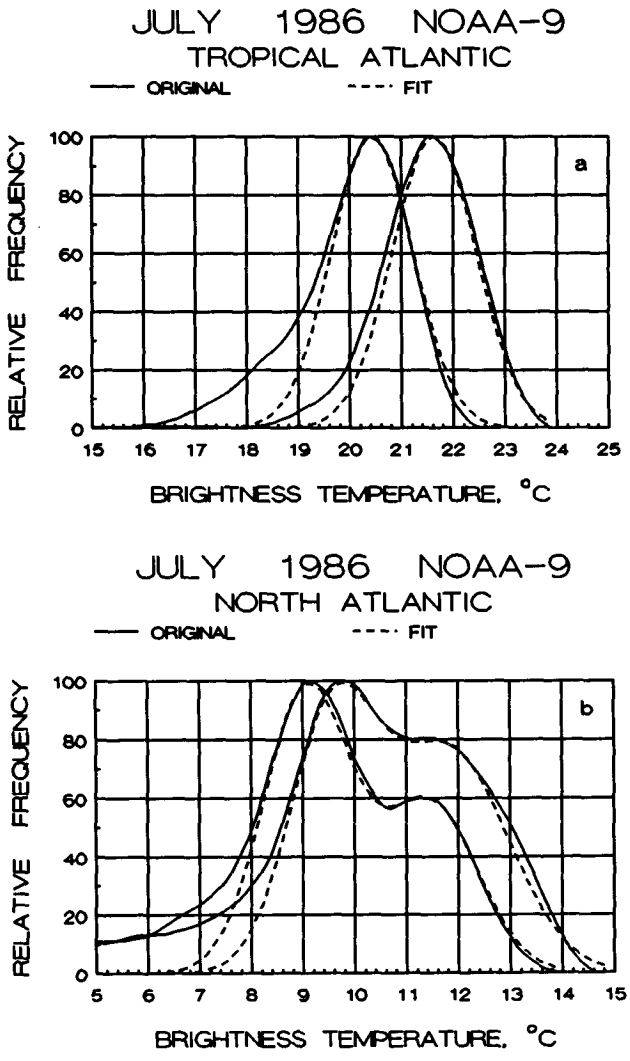


FIG. 2. Histograms of the *NOAA-9* AVHRR brightness temperatures in channels 4 (right curves) and 5 (left curves) in the near-nadir angular bin over the (a) tropical and (b) North Atlantic. Dashed lines show the results of their fitting by (bi)normal distributions.

TABLE 1. Empirical angular functions (°C) for the AVHRR channels 4 and 5 on board *NOAA-9* over the tropical and North Atlantic.

| Bin number | $m = \sec\Theta$ | Tropical Atlantic $\bar{t}_4$ + | Tropical Atlantic $\bar{t}_4$ − | Tropical Atlantic $\bar{t}_5$ + | Tropical Atlantic $\bar{t}_5$ − | North Atlantic $\bar{t}_4$ + | North Atlantic $\bar{t}_4$ − | North Atlantic $\bar{t}_5$ + | North Atlantic $\bar{t}_5$ − |
|---|---|---|---|---|---|---|---|---|---|
| ±1 | 1.1 | 21.7 | 21.7 | 20.5 | 20.7 | 9.6 | 9.5 | 9.1 | 9.1 |
| ±2 | 1.3 | 21.4 | 21.4 | 19.8 | 20.5 | 9.0 | 9.8 | 8.9 | 9.1 |
| ±3 | 1.5 | 21.2 | 21.0 | 18.9 | 19.8 | 8.1 | 9.0 | 7.0 | 8.5 |
| ±4 | 1.7 | — | — | — | — | 8.0 | 8.8 | 7.0 | 7.1 |
| ±5 | 1.9 | — | — | — | — | 7.9 | 8.3 | 6.7 | 6.7 |
| ±6 | 2.1 | 19.6 | 19.4 | 18.2 | 17.8 | 7.6 | 8.6 | 6.5 | 7.2 |
| ±7 | 2.3 | 19.1 | 19.4 | 17.7 | 17.8 | 7.3 | 7.8 | 6.1 | 6.5 |
| ±8 | 2.5 | 18.9 | 19.2 | 17.3 | 17.6 | 6.7 | 7.0 | 5.7 | 6.1 |
| ±9 | 2.7 | 18.5 | 18.8 | 17.0 | 17.2 | 6.7 | 6.7 | 4.3 | 5.3 |

tograms for different angle bins $\Delta_k$, $k = 1, \cdots, K$, provides $K$ points in the sought EAF, since all the mean values $\bar{t}(\Theta_k + \Delta\Theta_k/2)$ are associated with the mean ocean–atmosphere state $\bar{\mathbf{s}}$, which is assumed the same for different angle bins.

The question is which space–time scales $S$ and $\tau$ should be chosen. Although for statistics, the principle "the more the better" is used usually, the assumption of homogeneity holds progressively worse on large space–time scales, especially in regions with pronounced spatiotemporal variability of the ocean and atmosphere. Additionally, a compromise for the size of $(S, \tau, \Delta_k)$ domain should depend not only upon the degree to which the ocean and atmosphere are uniform, but also upon the spatial and temporal resolution in satellite data.

## 3. Data

In the present study, we use daily images from NOAA's global vegetation index (GVI) dataset (Kidwell 1990; Tarpley 1991) because these time series of radiances, uniformly mapped over the globe, are readily available. The GVI is a subsample of global area coverage (GAC) data collected from the afternoon overpasses of the NOAA satellites. The original 4-km GAC data are mapped into a plate Carree projection with a $0.15° \times 0.15°$ latitude–longitude resolution (one out of several GAC pixels within the GVI map cell is selected randomly). Since April 1985, this dataset consists of global maps of the AVHRR counts in channels 1, 2, 4, and 5, as well as the associated scan and solar zenith angles. The primary mission of the GVI dataset has been land studies. However, this paper demonstrates its potential for ocean studies if daily (not weekly composite) global maps are utilized.

In generating the GVI data, the 10-bit GAC counts in channels 4 and 5 are converted to radiances using a linear calibration procedure with the two coefficients calculated from periodic viewing of an onboard blackbody and deep space. The radiances are further converted to BTs ($T_4$ and $T_5$) and truncated to an 8-bit format (Kidwell 1990). This truncation results in a loss of accuracy: the GVI BTs are digitized with a step of 0.5°C for $t \geq -30$°C. The linear calibration procedure was shown to result in errors of up to 2°C because of nonlinearity of the sensor response (Weinreb et al. 1990). The nonlinearity correction depends upon the temperature of the internal target, which varies typically between 9° and 19°C and is not available in the GVI dataset. For this reason, we used the tabulated data of Weinreb et al. (1990) with the mean target temperature of 15.0°C to correct for the nonlinearity of the calibration. The error that may result from disregarding the variability of the target temperature rarely exceeds 0.5°C. The resulting absolute radiometric ac-

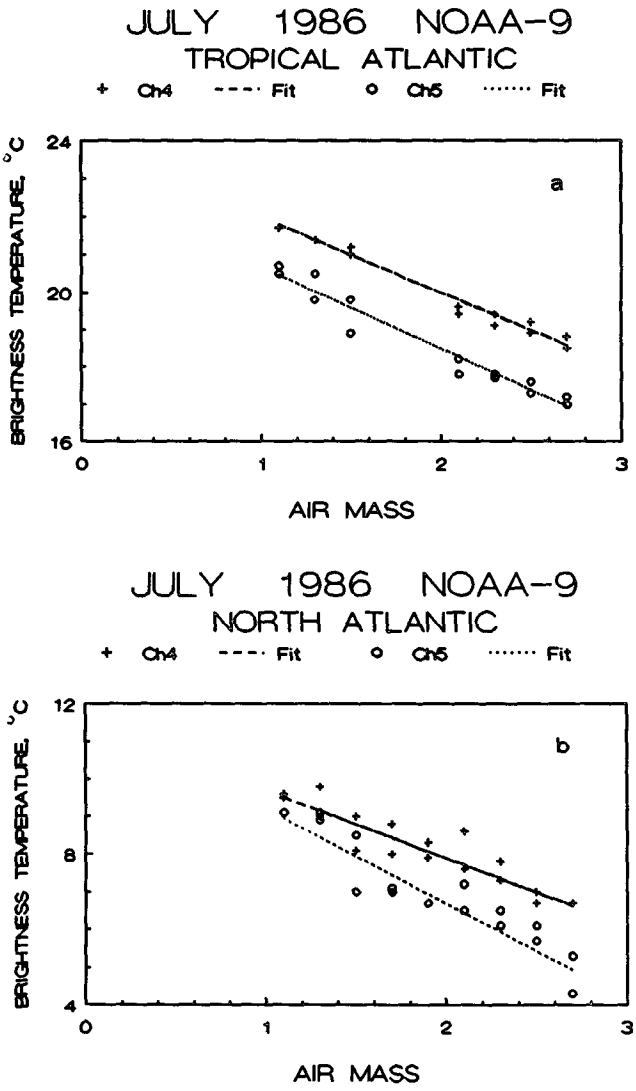


FIG. 3. The empirical angular functions of the brightness temperatures in AVHRR channels 4 and 5, and their linear fit over the (a) tropical and (b) North Atlantic.

TABLE 2. Statistics of linear approximation of the EAFs.

| | Channel | Regression | $R$ | $\sigma$ (°C) |
|---|---|---|---|---|
| Tropical Atlantic | 4 | $(23.95 \pm 0.85) - (2.00 \pm 0.09)m$ | 0.99 | 0.19 |
| | 5 | $(22.88 \pm 1.21) - (2.20 \pm 0.15)m$ | 0.97 | 0.32 |
| North Atlantic | 4 | $(11.51 \pm 0.76) - (1.78 \pm 0.18)m$ | 0.93 | 0.39 |
| | 5 | $(11.74 \pm 0.63) - (2.47 \pm 0.23)m$ | 0.94 | 0.50 |

curacy of such a calibration is estimated by Weinreb et al. (1990) to be about 0.55°C, which is compatible with the digitalization error.

The described satellite BT data are far from ideal for the estimation of the EAF because of low spatial resolution (an order of magnitude cruder as compared to GAC data, and two orders cruder as compared to LAC) and 0.5°C digitalization. The statistical nature of the procedure implies that the use of high-resolution data could improve the quantitative results of the present paper.

Thirty-one daily images from *NOAA-9* for July 1986 were processed over two regions: $S_1$ in the tropical Atlantic (10°–20°N, 40°–50°W—the same as used in ID94), and $S_2$ in the North Atlantic (50°–62°N, 10°–30°W). To estimate the homogeneity and stability over those regions, we used the U.S. Navy (1992) SST climatology, which provides the multiannual monthly means $t_c$ and standard deviations $\sigma_c$ within the $(1°)^2$ grid boxes. That climatology contains 121 of $(1°)^2$ boxes over the $S_1$, and 271 over the $S_2$, respectively. The histograms of $t_c - \bar{t}_c$ and $\sigma_c$ are shown in Fig. 1. The mean $\bar{t}_c$ over the $S_1$ and $S_2$ are 26.31° and 12.54°C, respectively.

The spatial nonuniformity of the SST field within the $S_1$ and $S_2$ is clearly seen from the width and shape of the histograms in Fig. 1a and is quantitatively described by standard deviations of 0.5° and 1.4°C, respectively. The region $S_2$ is significantly less uniform as compared to the $S_1$. Additionally, $S_2$ is extremely cloudy. The value of $\sigma_c$, which characterizes the year-to-year variability in the SST, is comparable in both regions: about 1°C over the tropical and 1.2°C over the North Atlantic. According to the U.S. Navy (1992), approximately 34% of the SST values can be expected between $\bar{t}_c$ and $\bar{t}_c + 1\sigma_c$; 14% between $\bar{t}_c + 1\sigma_c$ and $\bar{t}_c + 2\sigma_c$; and 2% between $\bar{t}_c + 2\sigma_c$ and $\bar{t}_c + 3\sigma_c$, and a mirror image is found on the negative side of the mean. One should bear that in mind when comparing the results of the SST retrieval with climatological values in the next section.

The total AVHRR swath width was subdivided into 18 angular bins (±9, symmetrically with respect to nadir) with an equidistant step of 0.2 in air mass $m$ = sec$\Theta$. Crude threshold cloud filters in channel 1, and spatial uniformity tests in channels 1 and 4 were used to exclude the most obvious clouds. Over the North Atlantic, these thresholds were set to 30%, 3%, and 2°C, respectively; in the Tropics, they were tightened to 20%, 2%, and 0.5°C. Note that the basic objective of the above cloud filtering is to clean up the peaks of the histograms to allow more reliable estimation of the position of the mode. An example of normalized smoothed histograms of the BTs over the $S_1$ and $S_2$ for one angle bin is shown in Fig. 2. Over the tropical Atlantic, the shape is close to a Gaussian—the result, close to that described in ID94. Over the North Atlantic, the two-peak shape indicates the presence of two clusters on the underlying surface. This feature is traced in almost every angle bin. We have fit this distribution with a binormal function and have chosen the more statistically significant colder cluster assuming it represents typical conditions for this region, whereas the warm peak most probably results from Gulf Stream intrusion.

## 4. Application of the empirical angular functions

The following relation approximates the angular function $t_i(\Theta)$ for aerosol-free atmosphere with a relatively low water vapor content and nonreflective sea surface (Prabhakara et al. 1974; McMillin 1975):

$$t_i(\Theta) \approx t_s - (t_s - \bar{t}_a)WK_i m(\Theta), \qquad (1)$$

where $\bar{t}_a$ is the effective temperature of the atmosphere; $K_i$ absorption coefficient; $m(\Theta)$ = sec$\Theta$ relative air mass of the atmosphere. According to (1), for a given ocean–atmosphere state ($\mathbf{s} = \{t_s, \bar{t}_a, W\}$ = const), $t_i(\Theta)$ may be approximated with a linear function of the air mass $m$. The SST can be estimated either by a formal extrapolation of $t_i(m)$ to zero air mass (Gorodetsky 1981; Chedin et al. 1982), or as a linear combination of the BTs in two channels

$$t_s = t_4(\Theta) + \alpha[t_4(\Theta) - t_5(\Theta)], \qquad (2)$$

where $\alpha = K_4(K_5 - K_4)^{-1}$ and does not depend on the angle $\Theta$ or the ocean–atmosphere state. The latter underlies the NOAA multichannel sea surface temperature (MCSST) algorithm (McClain et al. 1985)

$$t_s = \alpha_1 t_4(\Theta) + \alpha_2 t_5(\Theta) + \alpha_o. \qquad (3)$$

Dalu (1986) suggested retrieving $W$ as

$$W = A[t_4(\Theta) - t_5(\Theta)]\cos\Theta, \qquad (4)$$

where $A = [(K_{\lambda 5} - K_{\lambda 4})(t_s - \bar{t}_a)]^{-1}$ is assumed constant (=1.96 g cm$^{-2}$°C$^{-1}$).

The EAFs $t_4(\Theta)$ and $t_5(\Theta)$ enable one to check whether the linear approximation (1) holds and provides consistent intercepts in two channels, and whether the algorithms (3) and (4) result in angle-invariant SST and $W$.

## 5. Results and discussion

The results of the $\bar{t}(\Theta_k)$ derivation are given in Table 1. The histograms of two angular bins over the tropical Atlantic were extremely wide supposedly because of low warm clouds and have been excluded from the analysis. As one could expect, the results over the second target are less accurate because of pronounced nonuniformity of the underlying surface and persistent cloudiness.

Figure 3 shows the EAFs versus $m = \sec\Theta$, along with their linear fit. The statistics of the linear fits of the EAFs, including standard errors of the regression coefficients, are given in Table 2. The root-mean-square error of the retrieved EAFs is typically about 0.2°–0.3°C over the tropical (cf. with ID94), and 0.4°–0.5°C over the North Atlantic. In the Tropics, the results of linear extrapolation to zero air mass in channels 4 and 5 (24.0° and 22.9°C) differ both from each other and from the climatic SST (26.3°C) significantly. Over the North Atlantic, extrapolations to $m = 0$ (11.5° and 11.7°C) provide SST compatible with the climatic norm (12.5°C). The nonlinearity in the EAFs that may be responsible for the large extrapolation errors, seems to take place over both targets. However, this is compatible with the error level and cannot be analyzed in the present study.

Figure 4 shows residual angular effects in the SSTs retrieved using different operational NOAA daytime split-window algorithms (operationally, data with $\Theta < 60°$ only are used). During the *NOAA-9* lifetime, the MCSST equations have been changed several times (Kidwell 1991). For the present analysis, we have chosen the latest one implemented in the NOAA operations since 28 January 1988:

$$t_s = 3.608\, t_4 - 2.635\, t_5 + 0.33. \qquad (5)$$

In high latitudes, the MCSST eliminates the angular effect almost perfectly. In the Tropics, however, it underestimates the SST, with the discrepancy increasing with the viewing angle. The split-window EAFs are almost parallel here, and no angle-independent coefficients in linear retrieval algorithm (3) can provide here angle-invariant SST. This experimental result, which agrees well with that obtained in ID94 for the dual-window MCSST, has been already predicted theoretically by Llewellyn-Jones et al. (1984). They proposed the use of angle-dependent model coefficients $\alpha_i(m)$, calculated for AVHRR channels on board *NOAA-7*, for two samples of atmospheric situations representative for the North Atlantic and Tropics. We applied their coefficients to the respective EAFs from Table 2, for $m = 1$ and 2. The results are 24.7° and 24.3°C for the Tropics, and 10.8° and 11.4°C for the North Atlantic, respectively. One can see that in both cases the formulations of Llewellyn-Jones et al. (1984) treat angular dependence better than the MCSST.

With launch of *NOAA-11* in September 1988, a new generation of angle-dependent algorithms was implemented into NOAA operations specifically to improve retrievals in the Tropics, and to better treat the angle dependence. Here, we apply these algorithms to *NOAA-9* data to learn qualitatively if and to what extent they improve the retrieval. The following MCSST

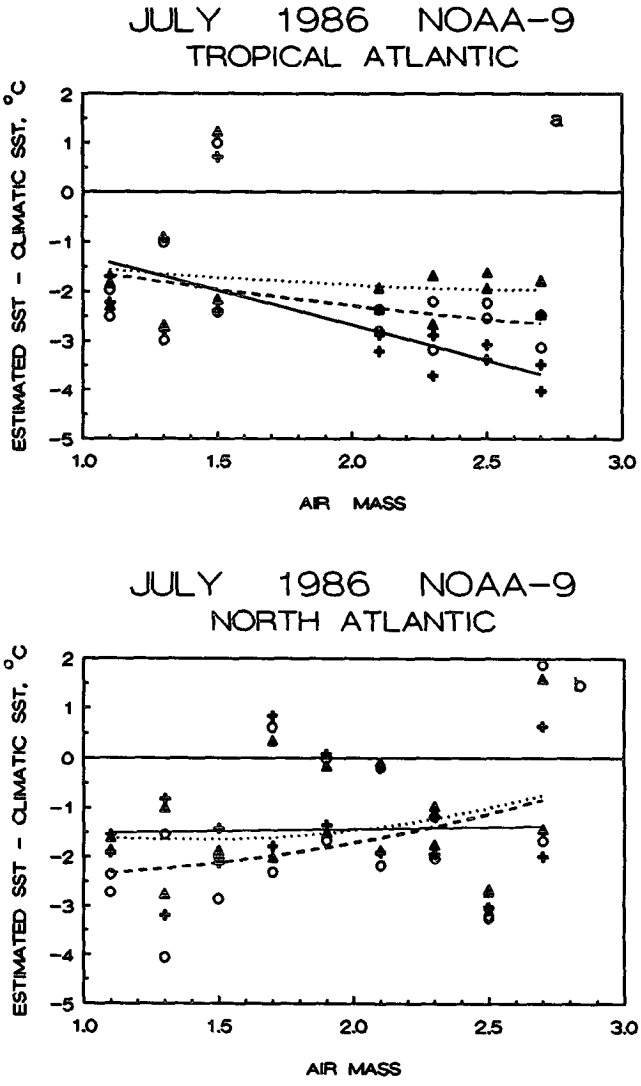


FIG. 4. Residual angle dependence in the retrieved SST over the (a) tropical and (b) North Atlantic. Solid line (+): the MCSST for *NOAA-9* [Eq. (5), operational from 28 January 1988 to 17 November 1988]. Dashed line (○): the MCSST for *NOAA-11* [Eq. (6), operational from 27 September 1989 to 18 April 1990]. Dotted line (▲): the CPSST for *NOAA-11* [Eq. (7), operational 18 April 1990 to present]. Detail description of the algorithms is given in (Kidwell 1991).

equation has been used in operations from 27 September 1989 (Kidwell 1991):

$$t_s = 1.013t_4 + 2.660(t_4 - t_5) + 0.527(t_4 - t_5)(m - 1) - 0.91. \quad (6)$$

Beginning 18 April 1990, a new cross-product SST (CPSST) algorithm has been implemented (Walton 1988; Kidwell 1991)

$$t_s = \frac{(0.191t_5 + 2.94)(t_4 - t_5 + 0.79)}{0.205t_5 - 0.173t_4 + 1.93} + 0.929t_5 + 0.81(t_4 - t_5)(m - 1) - 0.38. \quad (7)$$

Figure 4 shows that in the Tropics the newer operational algorithms successively improved the SST retrievals. It seems not to be the case over the North Atlantic. However, in both cases the amplitude of the residual angular effect is about 0.5°–1°C, which is already beyond the accuracy of the experimental data. Also, one should bear in mind that applying the nonlinear CPSST to the present EAFs is not a rigorous procedure. Rather, the CPSST algorithm should be applied to the original BTs, and the histograms of the retrieved SSTs plotted instead of BTs. This may be one of the reasons of the residual angle trend in the CPSST retrievals traced in Fig. 4. Note that the scatter in the retrieved SSTs is more pronounced as compared to the original EAFs. This is because SST retrieval algorithms significantly amplify any errors in the original BTs (see, e.g., Deshamps and Phulpin 1980). However, angular trends can still be analyzed even in such noisy data. The negative bias in all the satellite retrievals may result from inconsistency of the present calibration procedure with the operational ones, and difference between the AVHRR sensors onboard different satellites, and therefore it is not analyzed here.

Many different split-window algorithms for the SST retrieval have been suggested in literature (see, e.g., Deschamps and Phulpin 1980; Barton et al. 1989; Yokoyama and Tanba 1991; Antoine et al. 1992; Barton 1992; Emery et al. 1994). We leave it to the reader to check any of them in a manner described above using data from Table 2.

Similarly to the SST algorithms, one can check the algorithm (4) for the water vapor retrieval. Substituting the results of the EAFs fits from Table 2 into formula (4) for $m = 1$ and 2 yields $W = 2.50$ and 1.45 g cm$^{-2}$ in the Tropics, and 0.91 and 1.13 g cm$^{-2}$ over the North Atlantic. Dalu's (1986) algorithm, similar to the linear MCSST with angle-independent coefficients, seems to perform better in high latitudes. Unfortunately, at present we have no quantitative water vapor climatology in cloudless conditions to validate the above absolute values.

## 6. Concluding remarks

The EAFs allow one to check consistency of different angular methods for the SST retrieval in different spectral regions. Linear extrapolation of the split-window EAFs over the tropical Atlantic to zero air mass underestimates SST as compared to climatic norm in the region up to 2.5°C in channel 4 and 3.5°C in channel 5. One of the possible explanations of these errors may be nonlinearity of the EAFs that are not resolved in the present study because of insufficient accuracy of experimental data. For the North Atlantic, the results of extrapolation in both channels are close to the climatic SST.

Using the EAFs, one can check whether the algorithms for the SST and water vapor retrieval from a cross-scanning radiometer provide angle-invariant retrievals. We stress that the success of an algorithm in the EAF test does not mean necessarily that the algorithm is adequate. Results of testing the split-window MCSST (McClain et al. 1985) and water vapor (Dalu 1986) algorithms indicate that both fail to treat the angular effect in extremely moist conditions. Over the North Atlantic, they correct for the effect of variable observation geometry, although the absolute values of the SST and $W$ are yet to be validated.

Since the split-window EAFs are close to parallel in the Tropics, no angle-independent coefficients in a linear SST retrieval algorithm can provide angle-invariant retrievals. This result, which is in close agreement with that obtained by Ignatov and Dergileva (1994) for the same target in the tropical Atlantic using two independent datasets, supports the theoretical conclusion drawn by Llewellyn-Jones et al. (1984). Using their regionally adjusted angle-dependent coefficients in the linear SST retrieval algorithm allows one to eliminate the angle dependence in the retrieved SST with the accuracy of approximately 0.5°C.

Testing the newer MCSST and CPSST algorithms, which overtly incorporate the viewing angle dependence, has shown that both improve the SST retrievals in the Tropics. In high latitudes, however, they seem to overcorrect the angle dependence. This conclusion requires further checking since the amplitude of the residual error of about 0.5°–1°C is beyond the accuracy achieved in the present study.

More studies are needed, in different parts of the oceans, to better understand and correct for the angular effect. Applying the described statistical procedure to satellite data of higher spatial resolution and better radiometric accuracy is expected to enhance the accuracy of the EAFs, and the reliability of the geophysical conclusions drawn in this paper. Model and theoretical analysis of the angular effect is an important element of future studies.

*Acknowledgments.* Thanks go to Drs. G. Ohring and D. Tarpley (SRL) for a critical review of the manuscript. We are greatly indebted to P. Clemente-Colón (SRL) for providing the SST climatology, and to D. Sullivan (Research and Data Systems Corporation), who helped us in organizing the AVHRR time series

over the two oceanic targets. We acknowledge an anonymous reviewer, who proposed including analysis of the newer MCSST and CPSST algorithms and made other valuable suggestions. His arguments are reproduced almost literally in section 5. This work was done when A.I. held a National Research Council Associateship at the Satellite Research Laboratory, NOAA/NESDIS, on leave from the Marine Hydrophysics Institute, Sevastopol, Crimea, Ukraine.

## REFERENCES

Antoine, J. Y., M. Derrien, L. Harang, P. Le Borgne, H. Le Glau, and C. Le Goas, 1992: Errors at large satellite zenith angles on AVHRR derived sea surface temperatures. *Int. J. Remote Sens.*, **13,** 1797–1804.

Barton, I. J., 1992: Satellite-derived sea surface temperatures—A comparison between operational, theoretical, and experimental results. *J. Appl. Meteor.*, **31,** 433–442.

——, A. M. Zavody, D. M. O'Brien, D. R. Cutton, R. W. Saunders, and D. T. Llewellyn-Jones, 1989: Theoretical algorithms for satellite derived sea surface temperature. *J. Geophys. Res.*, **94**(D3), 11 587–11 601.

Chedin, A., N. A. Scott, and A. Berroir, 1982: A single-channel double-viewing angle method for sea surface temperature determination from coincident METEOSAT and *TIROS-N* radiometric measurements. *J. Appl. Meteor.*, **21,** 613–618.

Crosby, D. S., and K. S. Glasser, 1978: Radiance estimates from truncated observations. *J. Appl. Meteor.*, **17,** 1712–1715.

Dalu, G., 1986: Satellite remote sensing of atmospheric water vapor. *Int. J. Remote Sens.*, **7,** 1089–1097.

Deschamps, P. Y., and T. Phulpin, 1980: Atmospheric correction of infrared measurements of sea surface temperature using channels at 3.7, 11 and 12 m. *Bound.-Layer Meteor.*, **18,** 131–143.

Emery, W. J., Y. Yu, G. Wick, P. Schluessel, and R. Reynolds, 1994: Correcting infrared satellite estimates of sea surface temperature for atmospheric water vapor attenuation. *J. Geophys. Res.*, **99**(C3), 5219–5236.

Gorodetsky, A. K., 1981: Estimation of the surface temperature by the angular scanning method (in Russian). *Issledo. Zemli Kosmosa,* **2,** 36–44.

Holyer, R. J., 1984: A two-satellite method for measurement of sea surface temperature. *Int. J. Remote Sens.*, **5,** 115–131.

Ignatov, A. M., and I. L. Dergileva, 1994: Angular effect in the dual-window AVHRR brightness temperatures over oceans. *Int. J. Remote Sens.*, **15,** 3845–3850.

Kidwell, K., 1990: *Global Vegetation Index User's Guide.* U.S. Department of Commerce, National Oceanic and Atmospheric Administration, 49 pp.

——, 1991: *NOAA Polar Orbiter Users Guide.* U.S. Department of Commerce, National Oceanic and Atmospheric Administration, 200 pp.

Llewellyn-Jones, D. T., P. J. Minnett, R. W. Saunders, and A. M. Zavody, 1984: Satellite multichannel infrared measurements of sea surface temperature of the N.E. Atlantic Ocean using AVHRR/2. *Quart. J. Roy. Meteor. Soc.*, **110,** 613–631.

McClain, E. P., W. G. Pichel, and C. C. Walton, 1985: Comparative performance of AVHRR-based multichannel sea surface temperature. *J. Geophys. Res.*, **90,** 11 587–11 601.

McMillin, L. M., 1975: Estimation of sea surface temperatures from two infrared window measurements with different absorption. *J. Geophys. Res.*, **80,** 5113–5117.

Prabhakara, C., G. Dalu, and V. G. Kunde, 1974: Estimation of sea surface temperature from remote sensing in the 11- to 13-m window region. *J. Geophys. Res.*, **79,** 5039–5044.

Saunders, P. M., 1967: Aerial measurements of sea surface temperature in the infrared. *J. Geophys. Res.*, **72**(16), 4109–4117.

Smith, W. L., P. K. Rao, R. Koeffler, and W. R. Curtis, 1970: The determination of sea surface temperature from satellite high resolution infrared window radiation measurements. *Mon. Wea. Rev.*, **98,** 604–611.

Tarpley, J. D., 1991: The NOAA Global Vegetation Index product—A review. *Palaeogeogr. Paleoclim. Palaeoecol.*, **90,** 189–194.

U.S. Navy, 1992: Marine Climatic Atlas of the World. Naval Oceanography Command Detachment, Asheville, N.C., CD-ROM Ver. 1.0.

Walton, C. C., 1988: Nonlinear multichannel algorithms for estimating sea surface temperature with AVHRR satellite data. *J. Appl. Meteor.*, **27,** 115–124.

Weinreb, M. P., G. Hamilton, S. Brown, and R. J. Koszor, 1990: Nonlinearity corrections in calibration of Advanced Very High Resolution Radiometer infrared channels. *J. Geophys. Res.*, **95,** 7381–7388.

Yokoyama, R., and S. Tanba, 1991: Estimation of sea surface temperature via AVHRR of *NOAA-9*—Comparison with fixed buoy data. *Int. J. Remote Sens.*, **12,** 2513–2528.